A vitronectin-derived peptide reverses ovariectomy-induced bone loss via regulation of osteoblast and osteoclast differentiation

Seung-Ki Min[1,3], Hyun Ki Kang[2,3], Sung Youn Jung[2,3], Da Hyun Jang[2] and Byung-Moo Min[*,2]

Supplementary Results

Characterization of recombinant human vitronectin (rVn) truncations. To identify the biologically active domains that confer the cell functions exerted by vitronectin, three constructs covering the entire human vitronectin protein were generated (rVn-FI, rVn-FII, and rVn-FIII). A schematic diagram showing the rVn truncations of vitronectin, including the amino acid positions of their boundaries, is shown in Figure 1a. To provide convenient handles for subsequent protein purification and identification assays, all rVn fragments were expressed as histidine 6 (His_6)-tagged fusion proteins (Figure 1b). All three rVn fragments were purified to near homogeneity with Ni^{2+}-nitrilotriacetic acid (NTA) agarose under denaturing conditions, as determined by the Coomassie staining of an SDS-polyacrylamide gel (Figure 1b). rVn-FI was detected predominantly in the soluble fraction of the *Escherichia coli* lysates after the induction of protein expression, whereas rVn-FII and rVn-FIII were mainly present in the insoluble fraction. rVn-FI was therefore purified directly through Ni^{2+}-NTA affinity chromatography, whereas additional refolding processes were required for the purification of rVn-FII and rVn-FIII. The predicted molecular weights of rVn-FI, rVn-FII, and rVn-FIII were 32, 23, and 35 kDa, respectively; however, rVn-FI and rVn-FII migrated more slowly than expected for their predicted molecular weights (Figure 1b). This finding is consistent with a previous study that reported a significant difference between the predicted and observed mobility of an rVn fragment.[1] Based on mass spectrometric data, the actual size of the Vn1-97 fragment was 27.908 kDa,

although this fragment migrated with an apparent molecular weight of 42 kDa. This discrepancy may be due to many factors that affect protein migration, such as amino acid composition or an inconsistent charge-to-mass ratio in SDS-PAGE analysis.[2] To determine whether the rVn fragments formed intramolecular disulfide bonds, we subjected purified recombinant proteins to SDS-PAGE under either reducing or nonreducing conditions and investigated whether differences in mobility could be observed. The treatment of all three rVn fragments with 100 mM dithiothreitol prior to SDS-PAGE caused small but reproducible reductions in mobility, suggesting that intramolecular disulfide bonds were present in all three recombinant proteins (Figure 1c). Next, to assess the folding of the bacterially expressed rVn fragments, their secondary structures were assessed by circular dichroism spectroscopy. The circular dichroism spectra of the His_6–rVn fragments showed ellipticity minima at 208, 212, and 216 nm for rVn-FI, rVn-FII, and rVn-FIII, respectively (Figure 1d). These values are characteristic of a protein rich in β-structure, suggesting that the bacterially expressed rVn truncations were sufficiently folded to be able to perform their specific cell functions.

Cell functions of rVn truncations. As vitronectin is known to mediate cell attachment to various types of osteoblast-like cells,[1] each of the rVn truncations was examined for cell attachment activity. Human osteogenic cells adhered to rVn-FI and rVn-FII in a dose-dependent manner, but they did not adhere to rVn-FIII. The cell attachment activities of rVn-FI and rVn-FII reached a maximum level at ~5.7 $\mu g/cm^2$ in osteogenic cells (Figure 1e). As expected, human plasma vitronectin strongly promoted cell attachment, spreading, and migration in osteogenic cells (Figures 1f–h). Both rVn-FI and rVn-FII promoted greater cell attachment than the BSA control, although to a lesser extent than full-length vitronectin (Figure 1f). In addition, rVn-FI induced greater cell spreading and migration than the BSA control, whereas rVn-FII and rVn-FIII induced no cell spreading or migration (Figures 1g and h). These results suggest that rVn-FI was the most biologically active of the three recombinant truncations. However, we also identified significant cell attachment activity in rVn-FII, although this activity was weaker than that observed in rVn-FI.

Directed differentiation from SKPs to mesenchymal precursors to osteogenic cells. To isolate SKPs from human foreskin, skin samples composed of epidermis and dermis were dissociated and cultured in a defined medium containing fibroblast growth factor 2, epidermal growth factor, and leukemia inhibitory factor. Many cells adhered to the culture dishes and many died, but small spheres of floating cells formed within 3 days. These spheres were isolated, centrifuged, and separated into single cells with Accutase® treatment, which were transferred to a new flask 7 days after initial culturing. Again, many cells adhered, but cells in the floating spheres proliferated to generate larger spheres (Supplementary Figure S2a). The spheres were isolated after 7 days of culture, dissociated, and cultured in fresh medium supplemented with growth factors. Purified populations of floating spheres were obtained after three subcultures over three weeks using this process of selective attachment (Supplementary Figure S2a). Each time, the spheres were dissociated to single cells when passaged, and then subsequently proliferated to generate new spheres. After the isolation and expansion of the mesenchymal precursors from human foreskin, we identified an isolated population of homogeneous human mesenchymal precursors. The SKP-derived mesenchymal precursors were characterized by their ability to proliferate in culture with an attached, well-spread morphology (Supplementary Figure S2a) and by the presence of marker proteins on their surfaces (Supplementary Figure S2b). These expanded, attached SKP-derived mesenchymal precursors were uniformly positive for many surface proteins, including CD29, CD44, CD73, CD133, CD146, and Stro-1 (Supplementary Figure S2b). These results indicate that human SKPs can differentiate into SKP-derived mesenchymal precursors under the culture conditions described.

Osteogenic differentiation was induced in the SKP-derived mesenchymal cell cultures by treatment with β-glycerol phosphate, dexamethasone, and ascorbic acid in the presence of 10% FBS. The differentiated osteogenic cells formed aggregates or nodules, and calcium accumulation was evident after two weeks. Alizarin red S staining demonstrated that mineral deposits were associated with some of these nodules. These mineral deposits were abundant at two weeks and were localized

both to cells in the nodules and to some cells that grew in monolayers (Supplementary Figure S2c). qPCR analysis revealed an ~81-fold increase in *ALP* expression compared to the SKP-derived mesenchymal precursors (Supplementary Figure S2d). We then assessed the expression of osteogenic-specific markers, including RUNX2, bone sialoprotein, and osteocalcin, which previous studies have reported are intermediate or late markers of osteogenesis.[3] We found that the expression levels of RUNX2, bone sialoprotein, and osteocalcin were significantly upregulated in the differentiated osteogenic cells (Supplementary Figure S2d). We further confirmed the expression levels of osteogenic markers via RT-PCR, giving very similar results to those of the real-time RT-PCR analysis (Supplementary Figure S2e). Taken together, these results indicate that SKP-derived mesenchymal precursors can differentiate into an osteogenic lineage.

Supplementary Materials and Methods

Cell lines. The mouse embryo fibroblast NIH/3T3 cell line, the normal African green monkey kidney fibroblast CV-1 cell line, and the murine osteoblastic MC3T3-E1 cell line (ATCC, Rockville, MD, USA) were cultured in DMEM containing 10% fetal bovine serum. The PC12 cell line (ATCC), which was derived from a transplantable rat pheochromocytoma, was cultured in RPMI 1640 medium containing 10% FBS.

Construction, expression, and purification of human vitronectin truncations. Human vitronectin cDNA was cloned by RT-PCR using Superscript II Reverse Transcriptase, under conditions recommended by the manufacturer. mRNA isolated from Hep G2 cells was used for the template. All three fragments of human vitronectin (Vn-FI, Vn-FII, and Vn-FIII) were amplified by PCR using vitronectin cDNA as a template and were subsequently subcloned into the pGEM-T Easy Vector

System (Promega, Madison, WI, USA). The PCR primers used were as follows: Vn-FI, 5′-GGATCCGACCAAGAGTCATGCAAG-3′ (sense) and 5′-GAATTCTCAGGGCTGAGGTCTCC-3′ (antisense); Vn-FII, 5′-GGATCCCCAGCAGAGGAGGAGC-3′ (sense) and 5′-GAATTCTCACCAGAAGAGAAGCTCGAAG-3′ (antisense); and Vn-FIII, 5′-GGATCCGGCAGAACCTCTG-3′ (sense) and 5′-GAATTCTCACAGATGGCCAGGAGCTG-3′ (antisense). The resultant fragments were liberated with the appropriate restriction enzymes and were subsequently cloned into the *Bam*HI and *Eco*RI sites of the appropriate bacterial expression plasmid vector. Either pET-32a(+) (for rVn-FI and rVn-FIII; Novagen, Madison, WI, USA) or pRSET (for rVn-FII; Invitrogen) was used for recombinant expression. Correct insert orientation was verified by DNA sequence analysis. The recombinant expression and purification of truncated versions of vitronectin, including rVn-FI, rVn-FII, and rVn-FIII, were performed as previously described.[54] Briefly, the expression of recombinant proteins in *Escherichia coli* cells (BL21 strain) was induced with 1 mM isopropyl-*β*-D-thiogalactopyranoside for 5 h at 37 ℃. After protein induction, cells were harvested by centrifugation at 6,000 × g for 10 min. Cell pellets were resuspended in lysis buffer (50 mM NaH_2PO_4 and 300 mM NaCl, pH 8.0, for rVn-FI; and 8 M urea, 10 mM Tris-HCl, pH 8.0, 100 mM NaH_2PO_4, and 1 mM phenylmethylsulfonyl fluoride for rVn-FII and rVn-FIII). Recombinant rVn-FI was purified using a Ni^{2+}-NTA-agarose column (QIAGEN, Valencia, CA, USA) according to the manufacturer's instructions. Purified recombinant His_6-tagged truncations (rVn-FII and rVn-FIII) were further dialyzed sequentially into 3, 2, 1, and 0.5 M urea at pH 3.0. Finally, these proteins were dialyzed against PBS (pH 3.0) containing 1 mM phenylmethylsulfonyl fluoride. Protein concentrations were determined using the Bradford reagent.

Circular dichroism spectroscopy. Recombinant rVn proteins were prepared in PBS and diluted to 0.2 mg/ml. Circular dichroism spectra were recorded on a Jasco spectropolarimeter (model J-715; Jasco International, Tokyo, Japan). Protein samples were analyzed at 23 ℃, from 180 to 300 nm, with a 2-mm cell path length. Three repeated scans were averaged and smoothed by binomial curve

filtering. Molar ellipticities (in degrees·cm^2·$dmol^{-1}$) were calculated according to the protein concentration and molar mass of each rVn protein.

Migration sssay. Cell migration assays were performed with Transwell® migration chambers (pore size, 8 μm; Corning, Pittston, PA, USA). Briefly, the lower side of each Transwell filter was coated with vitronectin (0.23 μg/cm^2) or with rVn-FI, rVn-FII, or rVn-FIII (5.7 μg/cm^2) for 18 h at 4 ℃ and was then blocked with 1% BSA in PBS for 1 h at 37 ℃. Cells (2×10^5 cells/ml) were suspended in DMEM containing 0.5% FBS and 0.1% BSA. This suspension (100 μl) was seeded in the upper chamber of a Transwell filter. Cells were allowed to migrate for 24 h at 37 ℃. The cells were then fixed with 10% formalin for 15 min and stained with 0.5% crystal violet. Unmigrated cells, those remaining in the upper side of the Transwell filter, were removed with a cotton swab and counted under light microscopy. Cell migration was quantified by counting the number of cells that had migrated through the filter.

Cell viability assay. The viabilities of human osteogenic cells were investigated using the EZ-Cytox Cell Viability Assay Kit (water-soluble tetrazolium salt method). Osteogenic cells (3×10^3 cells/100 μl) were seeded onto a 96-well microplate, adapted for 48 h, and then treated with 50, 100, or 200 μg/ml VnP-16 for 24 or 48 h at 37 ℃. The water-soluble tetrazolium salt reagent solution (10 μl) was added to each well, and the plate was incubated for 2 h at 37 ℃. The absorbance at 450 nm was then measured using a microplate reader.

Flow cytometry. SKP-derived mesenchymal precursors were detached by trypsinization, and aliquots of 1.0×10^6 cells were prepared in 5-ml round-bottom test tubes. After rinsing with PBS containing 0.2% FBS, the cells were centrifuged and blocked with PBS containing 1% BSA and 0.2% FBS for 30 min at 4 ℃. The cells were then incubated with primary antibodies to CD29 (1:50; Chemicon), CD44 (1:25; BD Pharmingen, San Diego, CA, USA), CD73 (1:40; BD Pharmingen), CD133 (1:50;

Abcam, Cambridge, MA, USA), CD146 (1:1000; Abcam), and Stro-1 (1:17; Santa Cruz Biotechnology Inc.) for 1 h on ice. After washing with PBS containing 0.2% FBS, the cells were incubated with fluorescein isothiocyanate-labeled secondary antibodies for 1 h on ice. Finally, the cells were analyzed on a FACSCalibur flow cytometer (Becton-Dickinson, Franklin Lakes, NJ, USA).

qPCR and RT-PCR. Total RNA was isolated using the RNeasy® Mini Kit (QIAGEN, Valencia, CA, USA), according to the manufacturer's instructions. The cDNA was prepared using reverse transcriptase and a random hexamer, and PCR amplification of specific marker genes was performed using a final concentration of 300 nM for each primer (Supplementary Table S1) and a quantity of cDNA corresponding to 133 ng of total RNA. The PCR conditions were as follows: initial incubation at 95 ℃ for 2 min, followed by 30 cycles of 95 ℃ for 20 s, 60 ℃ for 10 s, and 70 ℃ for 4 s. The reaction products were analyzed by 1.5% agarose gel electrophoresis and visualized by ethidium bromide staining. The mRNA levels of specific marker genes were determined by qPCR. The primer sequences were designed using Primer Express® Software (version 3.0; Applied Biosystems). The cDNA was amplified using SYBR® Premix Ex Taq™ (Takara) with each primer at a concentration of 200 nM (Supplementary Tables S1 and S2), and a quantity of cDNA corresponding to 33 ng of total RNA. The quantitative PCR conditions were as follows: initial incubation at 95 ℃ for 30 s, followed by 40 cycles at 95 ℃ for 15 s, 60 ℃ for 20 s, and 72 ℃ for 34 s. The cycle threshold values were determined by automated threshold analysis using Sequenced Detection Software (version 1.3; Applied Biosystems), and then exported to Microsoft Excel for analysis. The relative expression level of each target mRNA was calculated using the comparative cycle threshold method, according to the manufacturer's protocol (Applied Biosystems).

Supplementary References

1. Anselme K. Osteoblast adhesion on biomaterials. *Biomaterials* 2000; **21:** 667-681.
2. Kamikubo Y, Okumura Y, Loskutoff DJ. Identification of the disulfide bonds in the recombinant somatomedin B domain of human vitronectin. *J Biol Chem* 2002; **277:** 27109-27119.
3. zur Nieden NI, Price FD, Davis LA, Everitt RE, Rancourt DE. Gene profiling on mixed embryonic stem cell populations reveals a biphasic role for β-catenin in osteogenic differentiation. *Mol Endocrinol* 2007; **21:** 674-685.

Supplementary Tables

Table S1. Primer sequences of the human osteogenic markers used for qPCR and RT-PCR.

Gene name (NCBI ID)	Forward primer	Reverse primer	Product size, bp
ALP (NM_000478.3)	5'- CCCACGTCGATTGCATCTCT-3'	5'- AGTAAGGCAGGTGCCAATGG-3'	100
RUNX2 (NM_001024630.1)	5'-GCCTTCAAGGTGGTAGCCC-3'	5'-CGTTACCCGCCATGACAGTA-3'	67
Bone sialoprotein (NM_004967.3)	5'- AAGGCTACGATGGCTATGATGGT-3'	5'- AATGGTAGCCGGATGCAAAG-3'	100
Osteocalcin (NM_199173.3)	5'-GAAGCCCAGCGGTGCA-3'	5'-CACTACCTCGCTGCCCTCC-3'	70
GAPDH (NM_002046.3)	5'- CCATCTTCCAGGAGCGAGATC-3'	5'- GCCTTCTCCATGGTGGTGAA-3'	100

Table S2. Primer sequences of the rat osteogenic markers used for qPCR.

Gene name (NCBI ID)	Forward primer	Reverse primer	Product size, bp
ALP (NM_013059.1)	5'-GGACCCTGCCTTACCAACTCA-3'	5'-GGAGTTTCAGGGCATTTTTCAA-3'	100
Bone sialoprotein (NM_012587.2)	5'-CAGCTGACGCTGGAAAGTTG-3'	5'-TCCTCGTCGCTTTCCTTCAT-3'	100
HPRT1 (NM_012583.2)	5'-GTTCTTTGCTGACCTGCTGGAT-3'	5'-TCCCCCGTTGACTGGTCAT-3'	120

Supplementary Figures

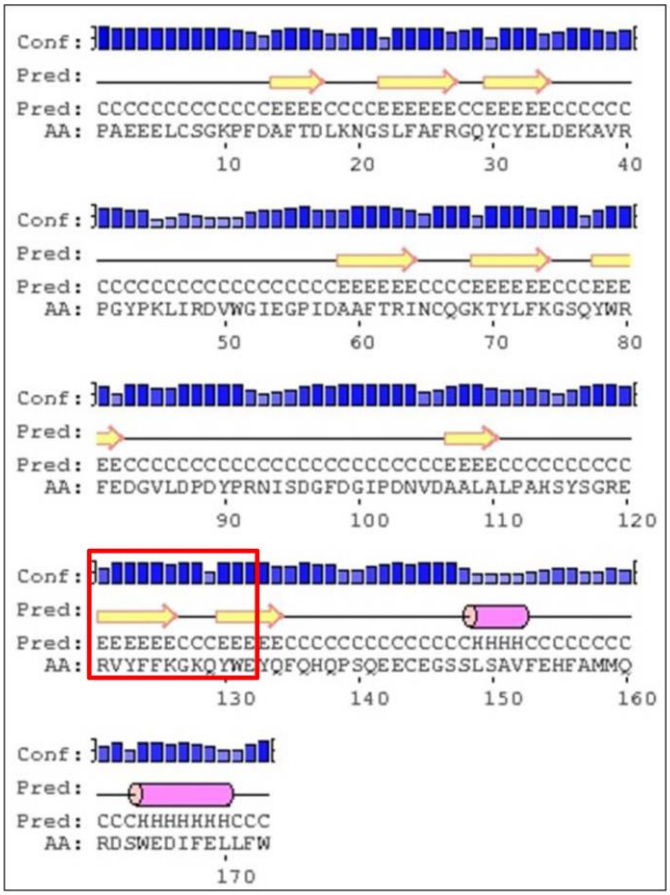

Figure S1 Predicted structure of the rVn-FII truncation. The structure was computed using the PSIPRED protein structure prediction server. The positions of the two α-helices (pink cylinders) and nine β-strands (yellow arrows) on the coil (black line) are indicated. The red box indicates the location of the VnP-16 peptide within the rVn-FII truncation. Conf, confidence of prediction; Pred, predicted secondary structure; AA, target sequence.

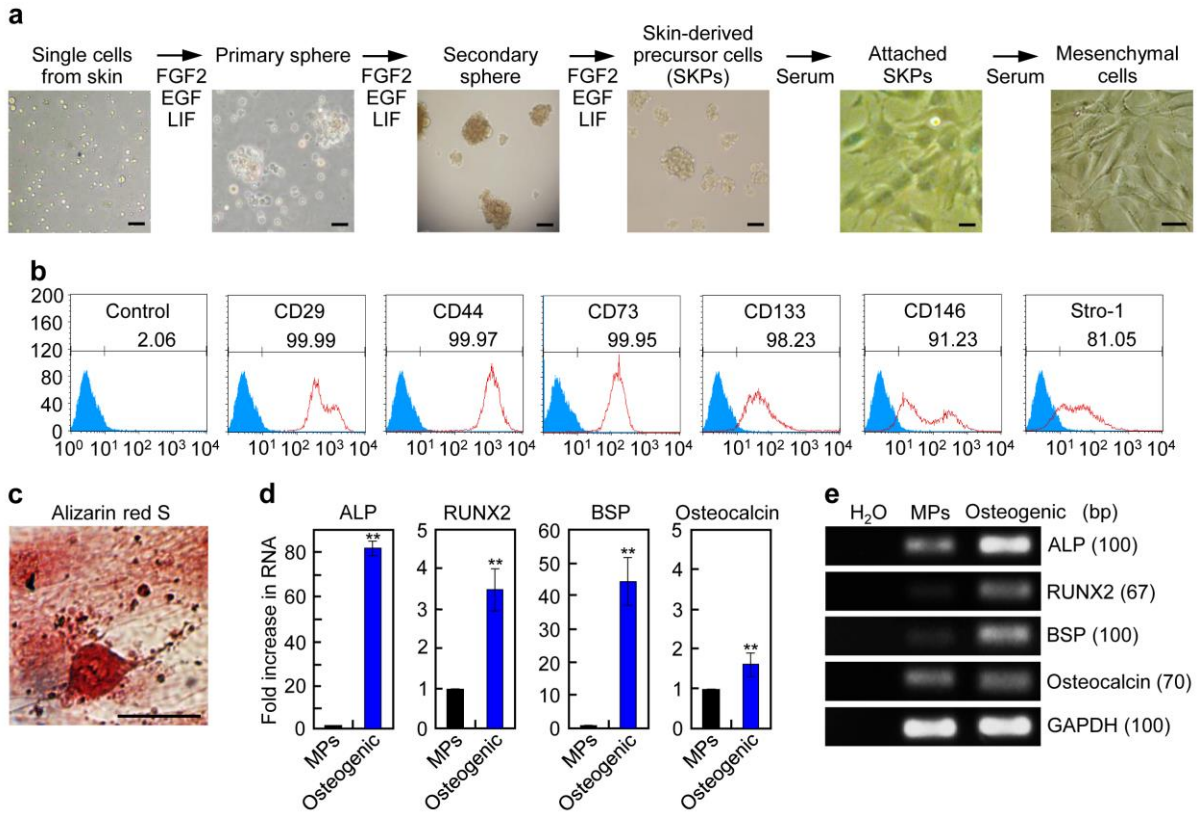

Figure S2 Characterization of mesenchymal precursors and osteogenic cells derived from SKPs. (**a**) Schematic illustration of the experimental design and representative images of sphere-forming SKPs following 7, 14, and 21 days of *in vitro* expansion. Following the initial purification, SKPs that grew as spheres in suspension were dissociated to single cells and regenerated over 1 week. Serum exposure led to the rapid conversion of SKP cultures into mesenchymal precursors. Scale bars, 50 μm. FGF2, fibroblast growth factor 2; EGF, epidermal growth factor; LIF, leukemia inhibitory factor. (**b**) Fluorescence-activated cell sorting analysis of the surface marker profiles of SKP-derived mesenchymal precursors. (**c**) Representative image of a monolayer culture of SKP-derived mesenchymal precursors after differentiation for 2 weeks under osteogenic conditions. The cells were stained for mineral deposits using Alizarin red S. Scale bars, 50 μm. (**d** and **e**) qPCR (**d**) and RT-PCR (**e**) analyses of the expression levels of osteogenic markers in the mesenchymal precursors (MPs) and osteogenic cells. A reaction without input nucleic acid was run in the first lane as a negative control. Data in **d** represent the mean ± SD (n = 4). $^{**}P < 0.01$. ALP, alkaline phosphatase; RUNX2, Runt-

related transcription factor 2; BSP, bone sialoprotein; GAPDH, glyceraldehyde 3-phosphate dehydrogenase; bp, base pair.

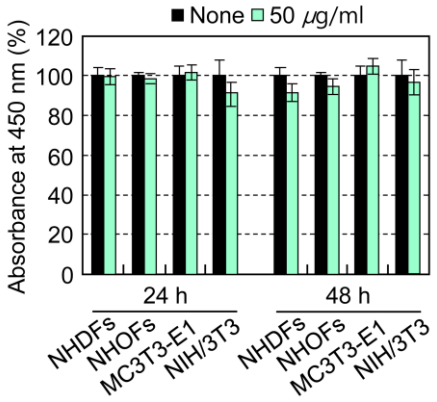

Figure S3 The viabilities of NHDFs, NHOFs, MC3T3-E1 cells, and NIH/3T3 cells treated with VnP-16 for 24 or 48 h.

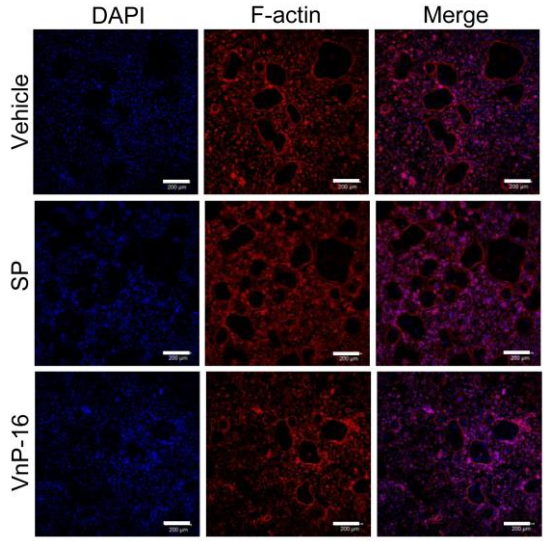

Figure S4 The effects of VnP-16 on F-actin-mediated cytoskeletal organization in mature osteoclasts. The osteoclasts were cultured for 1 day on plates precoated with vehicle (DMSO), SP (9.1 μg/cm^2), or VnP-16 (9.1 μg/cm^2), in the presence of 30 ng/ml M-CSF and 100 ng/ml RANKL. The cells were immunostained with DAPI (blue) and rhodamine-phalloidin (red). Scale bars, 200 μm.

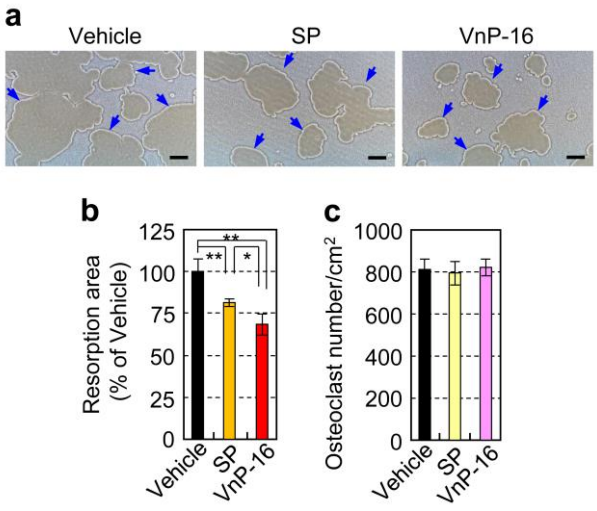

Figure S5 The effects of VnP-16 on the bone resorbing activity and survival of mature osteoclasts. (**a**–**c**) Mature osteoclasts were cultured for 24 h on Osteo Assay Surface plates coated with vehicle (DMSO), SP, or VnP-16 (9.1 μg/cm^2), in the presence of 30 ng/ml M-CSF and 100 ng/ml RANKL. (**a**)

The cells were removed and the resorbed pits (indicated by blue arrows) were photographed. Scale bars, 200 μm. (**b**) Bone resorption was assessed by pit area measurement. (**c**) After TRAP staining, the surviving osteoclasts were counted. Data in **b** and **c** represent the mean ± SD (n = 4). $^{*}P < 0.05$, $^{**}P < 0.01$.

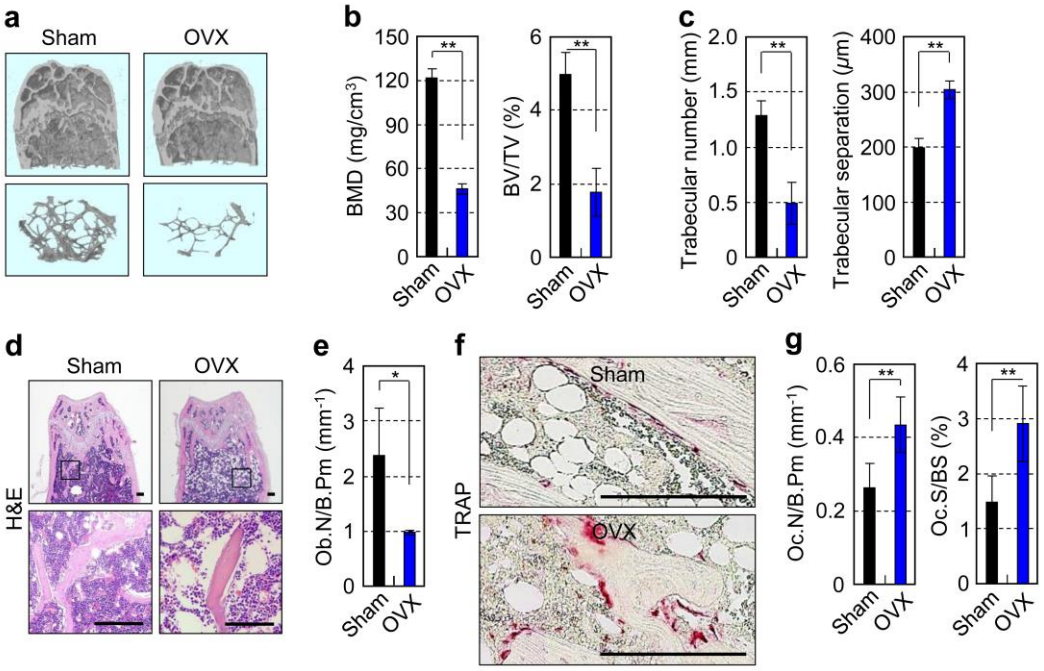

Figure S6 OVX mice exhibit severe trabecular bone loss in the femur. (**a**–**c**) μCT reconstruction of metaphyses of distal femurs (**a**), BMD and BV/TV (**b**), and trabecular number and separation in sham controls and OVX mice at 12 weeks after OVX. (**d**) H&E staining of femur sections from sham controls and OVX mice 12 weeks after OVX. Scale bars, 200 μm. (**e**) Morphometric analysis of osteoblast number in sham controls and OVX mice 12 weeks after OVX. (**f**) TRAP staining of femur sections from mice after OVX or sham operation. (**g**) Morphometric analysis of the osteoclast number and osteoclast surface in mice after OVX or sham operation. BS, bone surface. Scale bars, 200 μm. $^{*}P < 0.05$, $^{**}P < 0.01$.